

Full Length Article

Reaction gas induced activity enhancement for silver catalyst in ethylene epoxidation

Xiaojun Lu¹, Pei Zhang¹, Zhichao Deng, Chengyang He, Rui Zhang*

School of Chemical Engineering and Pharmacy and Key Laboratory for Green Chemical Process of Ministry of Education, Wuhan Institute of Technology, Wuhan 430205, PR China

ARTICLE INFO

Keywords:
 Ethylene epoxidation
 Silver catalyst
 Induction
 Carbonate species
 Subsurface oxygen

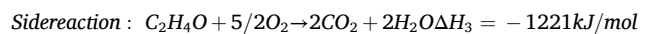
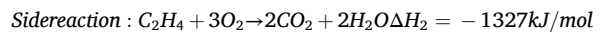
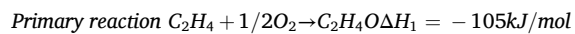
ABSTRACT

Ethylene oxide (EO) is an indispensable cornerstone chemical for producing industrial products such as cosmetics and pharmaceuticals. The Ag/ α -Al₂O₃ based ethylene epoxidation process is a successful method for producing EO on an industrial scale. However, achieving high production rates and selectivity for EO through catalyst preparation innovation has been challenging due to the elusive and non-unified reaction mechanism. In this study, a simple but effective induction procedure conducted at elevated temperatures (>260 °C) was found to enhance the activity of Ag/ α -Al₂O₃ for EO production. An 82 % increase of the EO production rate, from 1.19×10^{-2} to 2.17×10^{-2} mol/h/g_{Ag}, was achieved after induction at 260 °C. Suitable gas atmosphere (e.g., O₂, C₂H₄, and fully reactive gases) was found to be another requisite for successfully inducing the increase in the EO production rate. O₂-TPD analyses showed that more subsurface oxygen was generated in a suitable gas atmosphere compared to N₂. In-situ diffuse reflectance infrared Fourier transform spectroscopy results elucidate the formation of carbonates on the Ag surface after induction. The presence of carbonates stabilizes more subsurface oxygen, facilitating the adsorption and dissociation of O₂ and C₂H₄, thereby enhancing the reaction rate of the ethylene epoxidation process. The induced high activity could be maintained stably, as there was no sign of activity decrease over a 120-hour operation after induction. Due to the induced high activity, the Ag loading of the catalyst can be reduced in industrial applications, effectively lowering production costs.

1. Introduction

Ethylene is proposed as an important intermediate product in CO₂ electrocatalysis, the direct synthesis of olefins from syngas produced by renewable energy, and etc. The epoxidation of ethylene to produce ethylene oxide (EO) offers a pathway for large-scale application. EO is a key intermediate in the production of a wide variety of commercial products, including coolants, lubricants, paints, cosmetics, and pharmaceuticals [1–3]. About 72 % of EO is used to synthesis glycols, mainly monoethylene glycol (MEG), which is further polymerized to synthesis polyethylene terephthalate (PET) resin, the material from which most manufactured plastic containers are made [4–6]. The catalyst consisting of α -Al₂O₃ as the support and silver as the active component is the only widely used effective catalyst in the industrial production of EO [7,8]. Due to the moderate strength of the Ag—O bond [9] and the weak strength of the Ag—C bond [10], silver is an effective active component for ethylene epoxidation compared with Au, Cu, and other elements.

Selective ethylene oxidation and the side reactions are given by the following set of reaction equations:



Elucidating the action mechanism of oxygen species on Ag catalysts, as well as their reactivity and selectivity with ethylene, would enable the rational design of highly selective catalysts for ethylene epoxidation [11]. Oxygen atoms on the catalyst surface have been proposed to have two adsorption states, namely electrophilic oxygen atom and nucleophilic oxygen atom [12,13]. The C=C bond in the ethylene molecule is an electron-rich group, and the more electrophilic the molecules involved in the reaction are, the more they tend to attack the C=C bond in the ethylene molecule, which is favorable for the electrophilic

* Corresponding author.

E-mail address: ruizhang@wit.edu.cn (R. Zhang).¹ X.L. and P.Z. contributed equally to this paper.

reaction to form ethylene oxide [13–15]. Therefore, to improve the selectivity and reaction activity, more active oxygen species need to be generated through catalyst preparation and reaction engineering.

Previous study have suggested that the reaction activity and selectivity of pure silver catalysts are not ideal for the production of ethylene oxide [7]. Due to the sensitivity of the silver nanoparticle structure, it is prone to deactivation during the reaction, resulting in reduced reaction activity and selectivity. Therefore, appropriate catalytic promoters, such as rhenium (Re), cesium (Cs), chlorine (Cl), other transition metals, and alkali metals, were introduced to adjust the defects of the silver active sites for improving reaction activity and selectivity [16,17]. Cs is a key promoter to improve the selectivity of silver catalysts for ethylene epoxidation. Nielsen, Rochelle [18] found that adding a small amount of Cs to the silver catalyst can effectively improve the selectivity of the silver catalyst. Re can weaken the interaction between adsorbed oxygen and silver, promote the migration of adsorbed oxygen from the surface to the subsurface, and facilitate the formation of ethylene oxide [19]. Other studies found that the silver catalyst and Re promoter can increase the selectivity of ethylene oxide by about 5 %. The promoter Re mainly changes the chemical environment of the active sites, enabling the catalyst to activate more electrophilic oxygen and reduce the electron charge density of oxygen atoms [20,21]. Although the cost of the precious metal itself is high, its very low dosage, along with its ability to improve reaction efficiency, reduce raw material consumption, and extend catalyst life, can significantly reduce production costs and improve the overall economic efficiency of the ethylene epoxidation process. However, the addition of additives and modulation of surface oxygen properties can achieve a high selectivity with low activity. The simultaneous high activity and high selectivity Ag catalysts are still a challenge that needs to be solved.

Our previous study found that there was an abnormal increase in outlet EO content when the reaction temperature decreased from a stability test temperature of 260–230 °C compared with the control group at the same temperature [22]. This phenomenon led us to this study to pursue a simple method for obtaining a high activity with a high selectivity. In this study, we report an unusual activity improvement for the Cs and Re promoted silver catalyst in EO production with a simple yet very effective induction treatment. Two key parameters, temperature and inducing gas atmosphere, were studied thoroughly for induction for Re and Cs promoted silver catalysts. The particle size distribution of Ag on the surface of $\alpha\text{-Al}_2\text{O}_3$ was analyzed both before and after induction. Additionally, O₂-TPD and in-situ diffuse reflectance infrared Fourier transform spectroscopy (DRIFTS) were employed to elucidate the mechanism underlying the induction behavior. The proposed mechanism suggests that carbonates formed during induction stabilize subsurface oxygen species and enhance the adsorption and desorption of reaction gases, resulting in a significant improvement in reaction performance post-induction. The stability of the activity enhancement following induction was also investigated. This study provides valuable insights into reducing the catalyst cost in EO production.

2. Materials and methods

2.1. Catalyst preparation

Two different types of silver catalyst were prepared for the designed experiments, with the former containing Re and Cs as promoters and the latter consisting solely of silver. The catalyst with Cs and Re added was named Ag-Cs-Re/ Al_2O_3 , while the one without promoters was named Ag/ Al_2O_3 . Catalysts were prepared by vacuum impregnation using a silver amine complex (SAC) compound as the precursor. Silver nitrate solution was prepared by dissolving silver nitrate in deionized water. Meanwhile, a solution of ammonium oxalate was prepared by ammonium oxalate and deionized water at 50 °C. A precipitate of silver oxalate was then obtained by mixing these two solutions. Prior to filtration,

the precipitate was allowed to age for 30 min. The silver oxalate precipitate was washed eight times with deionized water and then dissolved in a solution composed of ethanolamine, ethylenediamine, and deionized water to prepare the SAC solution. The mass ratio of ethanolamine, ethylenediamine, and deionized water was set to 1:3:4. Finally, ammonium perrhenate and cesium sulfate were added to the SAC solution for wet impregnation on the $\alpha\text{-Al}_2\text{O}_3$ support. A mass ratio of 100:0.30:0.25 (2 g silver nitrate, 0.005 g ammonium perrhenate, and 0.004 g cesium sulfate.) was used for the elements of Ag, Re, and Cs in the impregnation solution.

The $\alpha\text{-Al}_2\text{O}_3$ support (3–4 mm in average diameter) was first vacuumed in a rotary evaporator during the wet impregnation. The impregnation solution (1:1 in $V_{\text{solution}}/V_{\text{pore}}$) was dripped onto the support holding in a flask on the rotary evaporator. Excess solvent was evaporated under a vacuum at 50 °C. The catalyst was then dried in an oven at 90 °C for 6 h after impregnation. The dried catalyst was calcined in a tube furnace with N₂ as a protecting gas. The temperature increased from room temperature to 330 °C at 4 °C/min during calcination and was maintained at the peak temperature for 5 min to allow for the decomposition of the precursors. Finally, the sample was cooled to room temperature and sealed for experiments and characterization. No other pre-treatment of the catalyst was performed prior to the experiment. Silver loading was controlled to 20 % when taking the mass of the support as 1, and the actual loading for each batch of catalyst preparation was determined by inductively coupled plasma (ICP) analysis (Table S1). The pure silver catalyst was prepared using the same procedure without adding promoters.

2.2. Catalyst characterization

The $\alpha\text{-Al}_2\text{O}_3$ support and the prepared silver catalyst were tested by a mercury porosimetry (Autopore IV9520, Micromeritics) to determine the pore properties, including the pore volume, average pore diameter, and specific surface area. The morphologies of the support and the loaded silver particles were analyzed by a scanning electron microscope (SEM). The number of particles counted for the particle size analysis was 350. The device used was Type JSM5510LV from Japan Electronics Corporation, with a resolution of 3.2 nm and a measuring voltage of 10 kV. The field emission sweep electron microscope (FESEM) was used to observe the size and dispersion of the silver nanoparticles in a better resolution. The equipment used was Gemini SEM300, with an acceleration voltage of 3 kV and a probe current of 3 pA–20 nA with a resolution of 0.7 nm at 15 kV.

X-ray diffraction (XRD) was used to determine the silver crystals and their facets for the fresh and used samples. The device used was D8 ADVANCE from Bruker, with an operating voltage of 40 kV and a current of 40 mA. A scanning rate of 5 °/min was applied to cover the scanning angle (2θ) of 20–90°. The crystal facets of the catalysts were identified by matching the collected diffraction pattern with the reference included in the Joint Committee on Powder Diffraction Standards (JCPDS) database.

The oxygen temperature programming desorption (O₂-TPD) analysis of the samples was carried out by using the automatic chemisorption instrument (AutoChem II 2920, Micromeritics). A 50–100 mg sample with a mesh size of 20–80 was placed in the reaction tube. After purging and drying, the sample was saturated with O₂ at 50 °C. The samples were heated at 10 °C/min from room temperature to 200 °C for drying pretreatment and were purged by He stream (30–50 mL/min) for 1 h. After cooling to 50 °C, desorption of the sample was carried out up to a temperature of 800 °C at 10 °C/min with He gas flow. The signal of exhaled gas was detected by a TCD.

2.3. Catalyst performance test

Experiments to investigate the performance of the catalyst were conducted in a fixed bed reactor with an inner diameter of 8 mm and a

length of 40 cm. At least 12 cm constant temperature for the catalyst loading region was achieved by three individually controlled heating elements along the reactor. The reaction temperature was monitored by a thermocouple located at the center of the catalyst bed. In each run, 1 g of 1–2 mm sized catalyst was diluted with silica sand three times in packing volume ($V_{\text{sand}}/V_{\text{cat}} = 3$) and loaded into the constant temperature region of the reactor. A widely industrial-scale EO project used feedstock gas composition was applied for all experimental runs, which consists of 28 % C_2H_4 , 7.5 % O_2 , 62.5 % N_2 , 2 % CO_2 , and 0.5 ppm $\text{C}_2\text{H}_4\text{Cl}_2$. The weight hourly space velocity (WHSV) of the feed gas was set at 4.2 L/h/g_{cat}, and the pressure was stabilized to 1.5 MPa by means of a back pressure regulator. The product and unreacted feedstock were depressurized to atmospheric pressure and sent to online gas chromatography (GC-8890 N, Agilent) equipped with two autosamplers and two detectors. Analysis of C_2H_4 and EO was carried out by FID, and permanent gases (O_2 , N_2 , and CO_2) were analyzed by TCD. The equations to calculate the conversion of the reactants, the EO selectivity, and the EO production rate are given in Part 1 in the [Supporting Information](#).

2.4. Induction experiments for the catalyst

To conduct the induction experiments, after the freshly charged catalyst was run at 230 °C until it reached a steady state, the reactor's temperature was set to the corresponding induction temperature (230 – 270 °C) while maintaining the same gas pressure, flow rate, and composition. An induction time of ten hours was selected to ensure that EO production during the induction process reached a steady state. In order to discover the essential factor, other than temperature, for the successful induction to high activity for the silver catalyst, a variety of atmospheres, including inert N_2 , reacting gas, C_2H_4 , and O_2 were employed to perform the induction experiments. Once the catalyst activity reached a steady state at 230 °C, the feed gas was switched to the selected single gas (e.g., N_2 , C_2H_4 and O_2) with nitrogen used as the balance gas, at the same operating pressure to initiate the induction process. At the same time, the temperature of the reactor was increased to 260 °C with a ramp rate of 5 °C/min. At the end of the induction period, the temperature was returned to the reaction temperature of 230 °C before the feed gas was switched to reaction gases, which had the same composition as the initial reaction gases.

2.5. In-situ DRIFTS experiment

In-situ diffuse reflectance infrared Fourier transform spectroscopy studies were conducted on a Bruker Invenio S infrared spectrometer equipped with an MCT detector for the promoted and unpromoted silver catalysts in an *in-situ* cell. Potassium bromide was added to the catalyst sample at a ratio of 30:1 ($m_{\text{KBr}}:m_{\text{catalyst}}$) and loaded into the sample holder. The procedure for *in-situ* DRIFTS experiments can be divided into three steps: adsorption and desorption before induction and adsorption and desorption after *in-situ* induction. The detailed procedure for the *in-situ* DRIFTS experiment is as follows. After loading the catalyst into the *in-situ* cell, the cell and the lines were purged with a mixture of air and C_2H_4 . The cell temperature was increased to 230 °C, and pressure increased to 1.5 MPa with a constant flow of air and C_2H_4 to allow the ethylene epoxidation to take place. After 4 h of reaction, the system was cooled down to 50 °C, and air (in another case, C_2H_4) was used to purge out the reactants and products for adsorption. Infrared signals were then measured for the O_2 adsorption at air pressure of 1.5 MPa and 50 °C and desorption under vacuum conditions at 50 and 300 °C, respectively. The *in-situ* cell was then subjected to the *in-situ* induction stage, during which the cell was operated at 260 °C and 1.5 MPa with a constant flow of a mixture of air and C_2H_4 for 5 h to allow the induction to occur. After induction, the specific adsorption procedure was the same as that for the sample before induction.

3. Result and discussion

3.1. Morphological and micro-structural properties of the catalyst

The porosity analysis results are shown in [Table 1](#). The support has a low specific surface area and a fair pore volume. After Ag loading, the values for pore feature parameters are reduced except for bulk density. The average pore size after silver loading remains large (450 nm), which, along with the low specific surface area of the $\alpha\text{-Al}_2\text{O}_3$ carrier, is suitable for ethylene epoxidation. This facilitates the mass transfer of the generated ethylene oxide into the bulk and reduces its deep oxidation to CO_2 .

The FESEM images and particle size distribution for the fresh Cs-Re/Ag/ Al_2O_3 catalyst and XRD analysis for both the fresh and the induced Ag-Cs-Re/ Al_2O_3 catalyst samples are presented in [Fig. 1](#). The high-resolution FESEM images show that $\alpha\text{-Al}_2\text{O}_3$ is bound together in a multi-directional lamellar structure with a size ranging from submicron to several microns and with a thickness of approximately 200–400 nm. The freshly prepared Ag-Cs-Re/ Al_2O_3 catalyst particles have an irregular prism-like surface and are loaded on the planes and edges of the support lamellae. The loosely bound state is one of the factors that causes the silver catalyst to migrate, aggregate, and form large particles at elevated temperatures or after long-term operation [47]. Statistical analysis using Nano Measurer software indicates that Ag particle diameters range from 100 nm to 280 nm, with a mean diameter of 195 nm. It's observed that, despite their large size, silver particles are well dispersed on the $\alpha\text{-Al}_2\text{O}_3$ support. Additionally, large silver catalysts are also commonly used in ethylene epoxidation reactions. [7,8].

The XRD result in [Fig. 1c](#) suggests that Ag remains at the state of Ag^0 for the Ag-Cs-Re/ Al_2O_3 catalyst samples before and after induction. Silver clusters are predominantly present on the most stable Ag (111) crystalline facet ([Fig. 1d](#)). The facets identified for Ag are consistent with the information included in JCPD #89-3722 and those reported in the literature [23]. The crystallite size of Ag suggested by Rietveld Refinement is 25–34 nm. These results indicate that Ag particles are in polycrystals with domain structure [24]. As shown in [Fig. 1d](#), the extensive peak overlap for fresh and induced Ag-Cs-Re/ Al_2O_3 catalyst samples suggests that the silver surface remains in the metallic state. However, the small peak shift of $\text{Ag}3d_{3/2}$ and $\text{Ag}3d_{5/2}$ from fresh and induced Ag-Cs-Re/ Al_2O_3 catalyst indicates an amount of silver oxide may exist on the surface, which originated from the oxidation of Ag at a high temperature during the reaction process.

The elemental mapping for the prepared Ag-Cs-Re/ Al_2O_3 catalyst is presented in [Fig. 2](#). It demonstrates that on top of the evenly distributed Al and O, the loaded silver is dispersed as particles in a diameter of several hundred nanometers. The distribution of silver and other elements shown by the elemental mapping is consistent with the FESEM image in [Fig. 1a](#).

3.2. Induced behavior

In our previous study, we observed that the activity of the Ag catalyst gradually increased during the reaction at a high operating temperature [22]. To investigate this behavior, we designed experiments with temperature and gas components as the main parameters.

Table 1
Porosity of support and catalyst.

Parameters	$\alpha\text{-Al}_2\text{O}_3$ support	Ag catalyst (Ag ^a on $\alpha\text{-Al}_2\text{O}_3$ support)
Total pore volume (mL/g)	0.57	0.32
Total specific surface area (m ² /g)	4.24	2.86
Median pore diameter (A, nm)	334.46	204.42
Average pore diameter (nm)	538.46	447.10
Bulk density (g/mL)	1.28	1.72
Porosity (%)	72.80	54.92

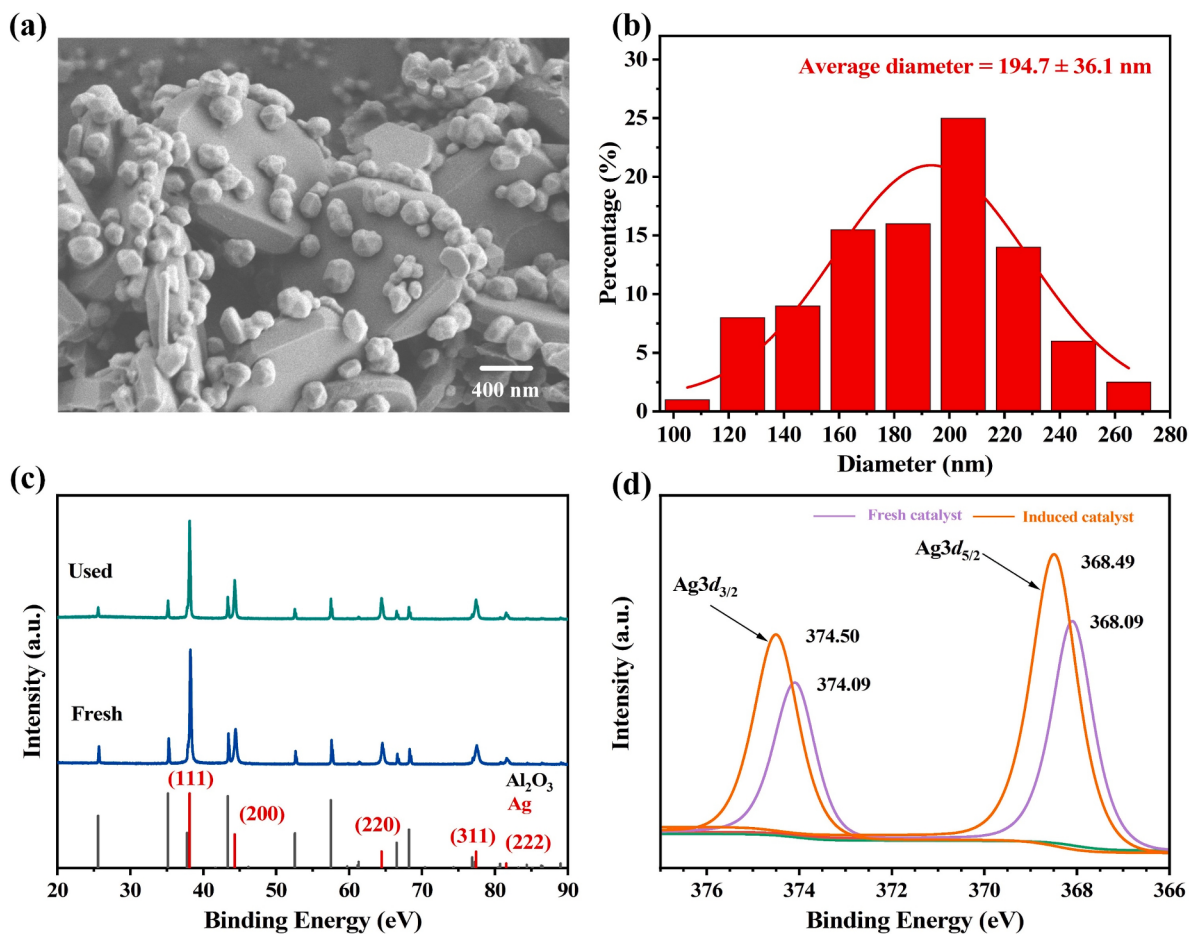


Fig. 1. Morphological and structural analysis for the prepared Ag-Cs-Re/Al₂O₃ catalyst: (a) FESEM image of the fresh Ag-Cs-Re/Al₂O₃ catalyst; (b) particle size distribution of the fresh Ag-Cs-Re/Al₂O₃ catalyst; (c) XRD diagram for the fresh and used Ag-Cs-Re/Al₂O₃ catalysts; (d) XPS result for the fresh and used Ag-Cs-Re/Al₂O₃ catalysts.

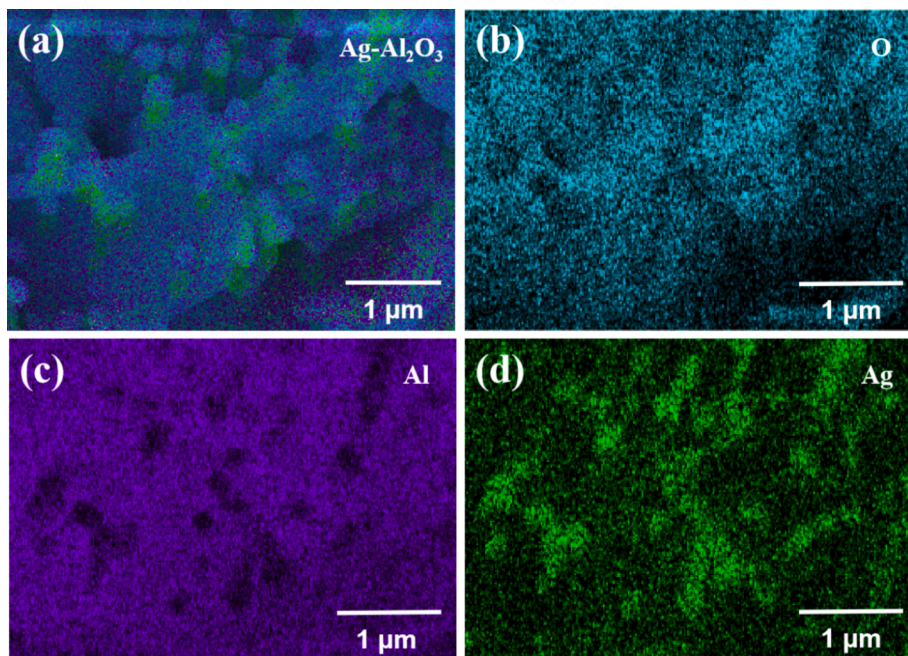


Fig. 2. Elemental mapping for the fresh Ag-Cs-Re/Al₂O₃ catalyst.

3.2.1. The effect of temperature on the induction behavior

Induction experiments were performed in the temperature range from 230 to 270 °C, a temperature range between the normal operating temperature (210–240 °C) for Ag-Cs-Re/Al₂O₃ catalysts and the decomposition temperature (>300 °C) during the preparation of the Ag-Cs-Re/Al₂O₃ catalyst. The reacting gas was directly employed as induced gas in this group of experiments. The induction results regarding the EO production, the C₂H₄ conversion, and the EO selectivity under different induction temperatures range from 240 to 270 °C are reported in Fig. 3. The production rate of EO gradually increased to a steady value of around 1.19×10^{-2} mol/h/g_{Ag} during the first 18 h. The EO formation rate increased as the induction phase began at a higher temperature than the reaction temperature of 230 °C. When the induction temperature was set to 250 °C, a rise of about 10 % in the EO production rate was observed. However, as the induction period ended at 28 h, the EO production rate decreased rapidly to a value similar to that before induction. When the induction temperature is raised to 260 °C, the induction phenomenon becomes significant, with an 82 % improvement in the EO production rate, from 1.19×10^{-2} to 2.17×10^{-2} mol/h/g_{Ag}. However, no further enhancement of the induction process was observed at an even higher temperature (270 °C). Instead, the activity was suppressed compared to the results obtained by induction at 260 °C. It can be concluded that temperature is the essential factor for the induction behavior to occur, while relatively low temperatures (below 250 °C) do not lead to the observed induction behavior.

The C₂H₄ conversion results during induction, as well as the pre-and post-induction reactions shown in Fig. 3b, correspond to EO production rate results shown in Fig. 3a. When the induction temperature was set to

260 °C or 270 °C, the conversion of C₂H₄ almost doubled the value before induction. The C₂H₄ conversion following induction at 250 °C shows even a slight decrease while the EO formation rate has improved slightly. It indicates that the EO selectivity increased after the induction process.

Besides the improvement in EO production activity caused by induction at elevated temperatures, the selectivity of the Ag-Cs-Re/Al₂O₃ catalyst for EO was also improved, as shown in Fig. 3c. Among the investigated temperatures, 250 °C benefits EO selectivity the most, increasing it from 83.5 % to 88 %. However, it improves the EO reaction rate the least (Fig. 3a). The EO selectivity has increased by a constant value about 87 % after the induction at 250–270 °C. Meanwhile, the selectivity of EO (Fig. 3c) shows a decrease during the induction period, indicating that higher temperatures intensified the reaction rate of EO while favoring the deep oxidation of ethylene.

These collective experiments confirm that a sufficiently high temperature is essential to initiate the induction effect on Ag-Cs-Re/Al₂O₃ catalysts to achieve a higher EO production rate. When the reaction rates obtained after induction are plotted as a function of induction temperature, as shown in Fig. 3d, we could determine a turning region with respect to temperature to induce a significant increase in EO activity. Moreover, the experimental results indicate that the optimal induction temperature is around 260 °C and that an induction temperature beyond this does not further benefit the EO production activity.

3.2.2. The effect of the atmosphere on the induction behavior

Temperature is a prerequisite for higher activity by causing the Ag-Cs-Re/Al₂O₃ catalyst to undergo induction behavior. The previous

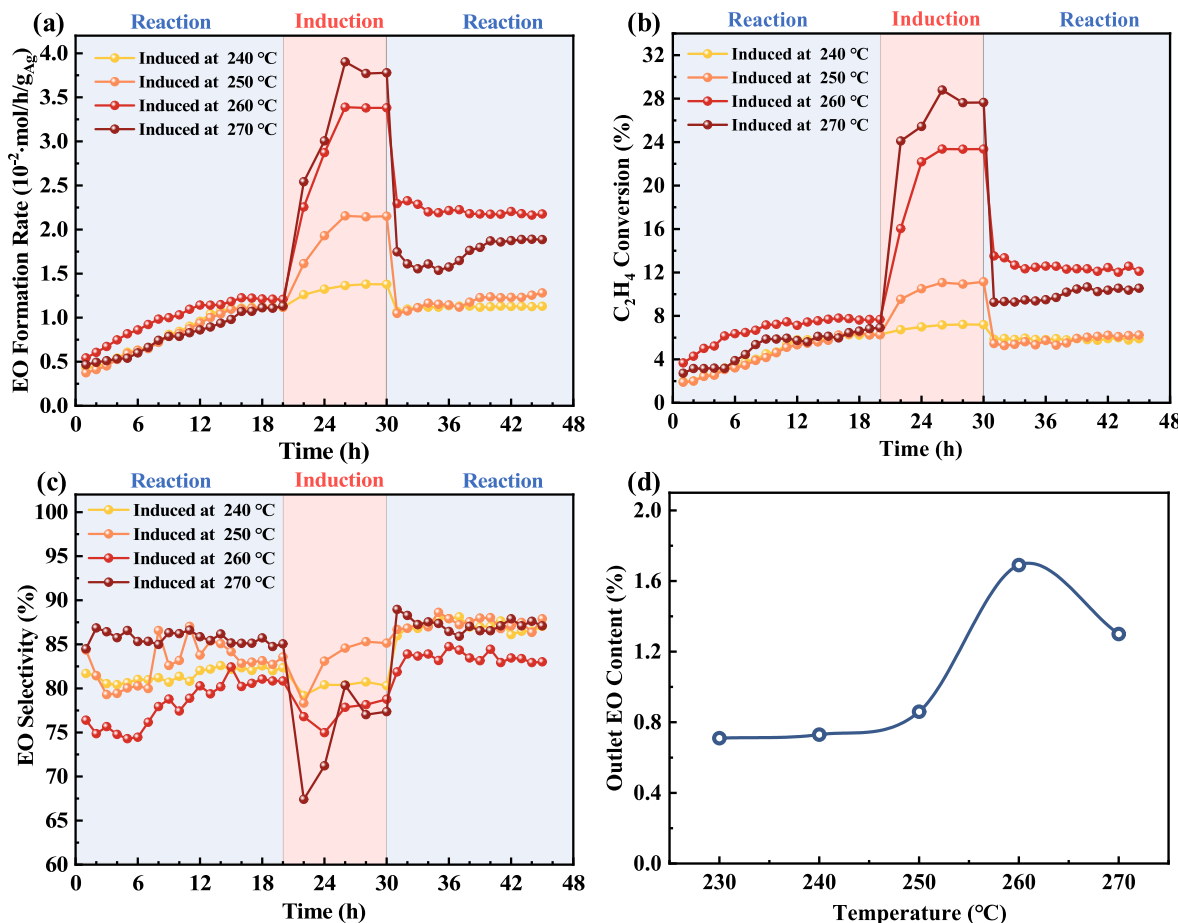


Fig. 3. Time courses of (a) EO formation rate, (b) EO selectivity, (c) C₂H₄ conversion, and (d) outlet EO content before and after induced at different temperatures for ethylene epoxidation catalyzed by Ag-Cs-Re/Al₂O₃ catalyst at reaction conditions of 230 °C, 1.5 MPa C₂H₄, 1.5 MPa O₂ and a gas hourly space velocity of 4200 mL·h⁻¹·g_{Ag}⁻¹.

observation when we first discovered the induction behavior led us to deduce that temperature may not be the only factor facilitating such a phenomenon. Therefore, we used three single gases (ethylene, oxygen and nitrogen) to study the effect of gas atmosphere on the induction effect. An optimal induction temperature of 260 °C and an induction time of 10 h were employed, whereas the pre- and post-induction reaction temperature was maintained at 230 °C for all experimental runs.

As shown in Fig. 4a, induction behavior for increased EO activity could not be achieved using the inert gas N₂, as the activity of the Ag-Cs-Re/Al₂O₃ catalyst remained unchanged at an EO formation rate of 1.19×10^{-2} mol/h/g_{Ag} before and after the induction period at 260 °C. It was also observed that the improved activities by induction could be achieved by using either or both of the reaction gases, O₂ and C₂H₄, with EO production activity nearly doubled. It should be noted that the O₂-induced EO formation rate is higher than that induced by C₂H₄ despite being very close before induction, suggesting that O₂-induction may result in a better effect on enhancing EO activity. Although the focus is on the EO activity at the steady state of the Ag-Cs-Re/Al₂O₃ catalyst after induction, the data in the transient period between the end of the induction phase and the formation of the following steady state has also attracted our attention. If only one of the reaction gases is used for induction, the overall rate of EO generation will increase before a new steady state is established, primarily because of the lack of EO in the reactor system during the induction period, whereas with the use of the full reacting gas the originally existing high EO concentration in the reactor system has to be replaced by a low EO concentration, i.e., it changes from a high to a stable EO concentration state.

The C₂H₄ reaction rates presented in Fig. 4b show a trend similar to that of the EO contents in the outflow streams. There were no changes in their pre- and post-induction values by N₂, but significant changes were observed when the Ag-Cs-Re/Al₂O₃ catalysts were induced by O₂, C₂H₄, or a mixture of these gases. The C₂H₄ conversion following O₂ induction is at the lowest level of the three successful induction results, suggesting that less C₂H₄ underwent deep oxidation to form CO₂ when combined with the data in Fig. 4a.

In addition, the difference in induction behavior caused by the different gases is pronounced in the selectivity of the EO product, as shown in Fig. 4c. Induction by N₂ had no observable effect on product selectivity, although Ag-Cs-Re/Al₂O₃ catalyst particles did become larger during the induction process (see Fig. 5 below). Induction with pure C₂H₄ led to a slight decrease in EO selectivity from 82 % prior to induction to 80.5 % post-induction. In contrast, induction with oxygen and the complete reaction gases both increase the EO selectivity from 80 % to 85 %. The higher selectivity for EO is thus closely related to the gas used during the induction process. When induction is carried out with gases containing oxygen, the role of oxygen may be prominent compared to other gases. Oxygen adsorbed on the surface of the Ag-Cs-Re/Al₂O₃ catalyst may facilitate the formation of active species, such as subsurface oxygen, during the reaction, resulting in higher EO selectivity [25].

With the result in this section and above regarding induction temperature, it can be seen that both temperature and gas conditions are necessary for induction to be effective. A sufficiently high temperature alone does not initiate the induction process or increase EO activity, as

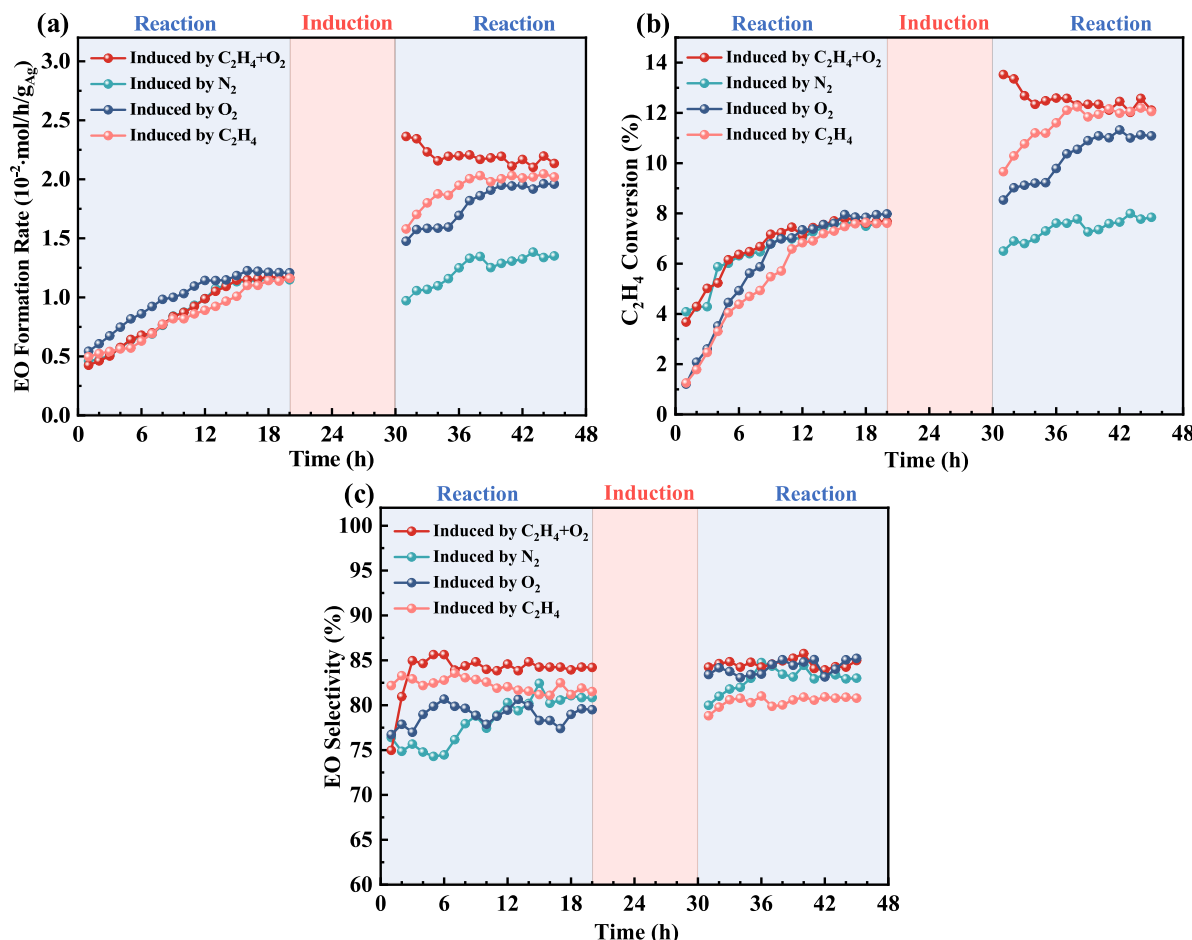


Fig. 4. Time courses of (a) EO formation rate, (b) EO selectivity, and (c) C₂H₄ conversion before and after induced at 260 °C under different atmospheres for ethylene epoxidation catalyzed by Ag-Cs-Re/Al₂O₃ catalyst at reaction conditions of 230 °C, 1.5 MPa C₂H₄, 1.5 MPa O₂ and a gas hourly space velocity of 4200 mL·h⁻¹·g_{Ag}⁻¹. When one single gas was used during the induction period, no reaction data are available for the induction period.

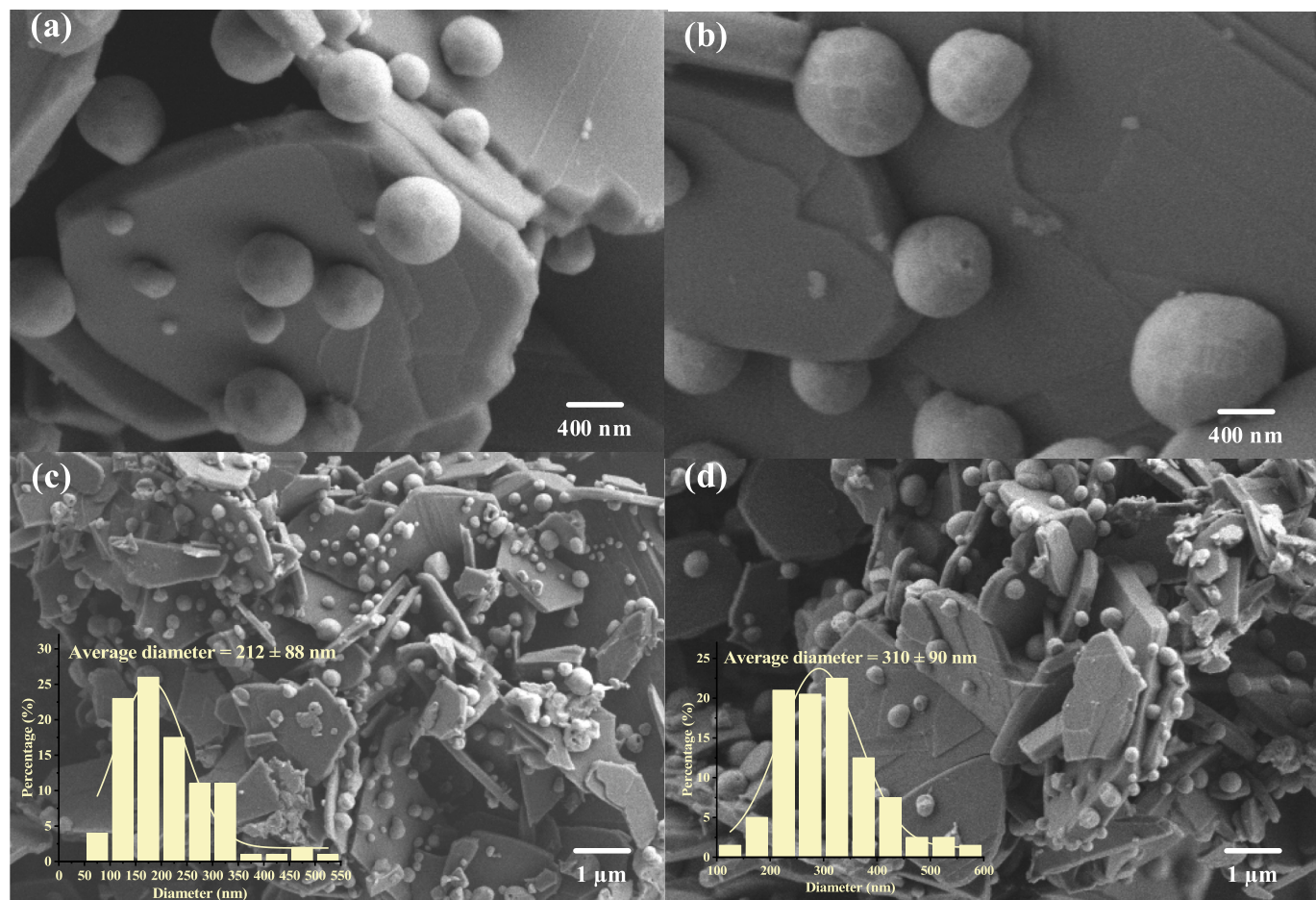


Fig. 5. FESEM images of Ag-Cs-Re/Al₂O₃ catalyst after induced by (a) reacting gas and (b) N₂ at 260 °C; Particle size distribution of Ag/α-Al₂O₃ after induced by (c) reacting gas and (d) N₂ at 260 °C.

demonstrated by the inability of N₂ to achieve an induction effect. Induction with O₂-containing gas is necessary to enhance EO selectivity. However, the mechanisms behind the increase in EO generation rate and selectivity remain unclear based on existing literature. Therefore, we further explore this phenomenon using advanced characterization techniques such as O₂-TPD and DRIFTS.

3.3. Exploring the induction mechanism

3.3.1. The morphology of the catalyst after induction

To examine the morphological properties of the Ag-Cs-Re/Al₂O₃ catalysts after the reaction-induction-reaction process with different gas atmospheres, FESEM analysis was performed on two Ag-Cs-Re/Al₂O₃ catalysts: one induced with fully reacting gas and the other with N₂. The results and their particle size distributions are shown in Fig. 5. Compared with the FESEM images before and after induction, it was found that the silver particles changed from an irregular prism-like shape to a spherical appearance. This demonstrates that rearrangements occurred on the surface of the silver particles under the reaction conditions. Although a low temperature could not achieve successful induction, it still led to the rearrangement of Ag particles during the reaction, as noted in the previous study [26]. Therefore, we hypothesize that the rearrangement of the silver particle on the α-Al₂O₃ surface is not the key factor to achieve the induction effect.

Even though the Ag-Cs-Re/Al₂O₃ catalyst samples were run at the same temperature and duration (reaction + induction), the silver particles on α-Al₂O₃ exhibited differences in size distribution and average diameter. After induction, particle sizes larger than 280 nm (the up limit

of the particle size for the fresh Ag-Cs-Re/Al₂O₃ catalyst) appeared for both samples. Once induction to a higher EO rate was successfully achieved by treating the Ag-Cs-Re/Al₂O₃ catalyst with the reacting gas at a temperature higher than 250 °C, a slight aggregation of silver particles was observed, with an average particle size of 210 nm. Where no improvement in EO activity was obtained with the induction procedure under N₂ gas atmosphere, the average silver particle size has increased to 310 nm with a broader size distribution. The aggregation of silver particles leading to the growth of silver particles is thought to be one of the causes of Ag-Cs-Re/Al₂O₃ catalyst deactivation, particularly the decrease in the EO formation rate [27]. Moreover, previous work has shown that with the growth of silver particles, the rate of the primary reaction (ethylene epoxidation) decreases while the rate of the secondary reaction (deep oxidation of C₂H₄ to form CO₂ and H₂O) increases significantly, resulting in a decrease in the selectivity of the EO [28,29]. The FESEM results obtained here suggest that the growth rate of silver particles may be attenuated when exposed to the reacting gases.

3.3.2. O₂-TPD analysis of induced catalysts

Oxygen activation on the catalyst surface plays an important role in the ethylene epoxidation reaction, and O₂-TPD is one of the most effective techniques for studying the oxygen adsorption and activation capacity of catalysts. Molecularly adsorbed oxygen is resolved on the silver surface at relatively low temperatures, while lattice oxygen occurs at 750 °C [30]. And the oxygen resolved at 200–500 °C is usually considered to be the active oxygen species on silver, which are classified as nucleophilic, electrophilic, and subsurface oxygens [31–34]. The O₂-TPD results for the Ag-Cs-Re/Al₂O₃ catalyst induced by different single

gases are shown in Fig. 6. The nucleophilic, electrophilic, and subsurface oxygen ratios were found by fitting are N₂ (36:46:18), O₂ (49:9:42), and C₂H₄ (33:22:45), respectively. It was clearly found that the percentage of subsurface oxygen induced through oxygen and ethylene was much higher, so induction through these two gases showed significantly higher activity. It was further found that although the nitrogen-induced Ag-Cs-Re/Al₂O₃ catalyst had a high content of nucleophilic oxygen, the reaction data showed that its activity was not as good as that of the oxygen and ethylene-induced Ag-Cs-Re/Al₂O₃ catalysts, which also confirmed that subsurface oxygen was more active than electrophilic oxygen for the epoxidation of ethylene. Therefore, more subsurface oxygen was generated on the surface of the Ag-Cs-Re/Al₂O₃ catalysts induced by oxygen and ethylene, which was more favorable for the reaction.

3.3.3. In-situ DRIFTS analysis

Based on the O₂-TPD results indicating that more active oxygen species were obtained through the induction process, in situ DRIFTS analysis was further applied to reveal the high reactivity and the behavior of the Ag/α-Al₂O₃ surface. The infrared spectra of fresh Ag-Cs-Re/Al₂O₃ catalysts before and after in situ induction with reacting gases in the cell were obtained (Fig. 7). Two infrared vibrational peaks appeared simultaneously at 1754 cm⁻¹ and 1273 cm⁻¹ after induction, corresponding to the vibrational characteristic peaks of C=O and C—O [35,36]. This suggests the formation of new species on the Ag-Cs-Re/Al₂O₃ catalyst surface during the induction process, possibly carbonates, acetates, or oxalates. Further observation of the spectrum of the induced Ag-Cs-Re/Al₂O₃ catalyst after O₂ adsorption at 300 °C revealed that these species remained stable at high temperatures. Considering that oxalates and acetates cannot exist stably at 300 °C [37], these species are highly likely to be carbonates, which can remain stable at high temperatures. This is consistent with the formation of carbonate on the Ag particle surface observed during the reaction in previous studies [35,38]. Therefore, we can conclude that the intermediate products generated in the EO production process, aldehyde, may form a stable carbonate structure on the Ag surface at high temperature during the induction process. The formation and accumulation of carbonates are more favorable under certain pressure and temperature conditions. Besides, The peak intensity enhancement after induction at 1421 cm⁻¹ may also be attributed to newly generated C—O bond vibrations of monodentate and bidentate carbonate [39], the peak at 1421 cm⁻¹ of the sample before induction may correspond to the remaining nitrate in

the preparation of Ag/α-Al₂O₃.

DFT calculations in previous studies have shown that carbonates stabilize more subsurface oxygen, which alters the electronic structure of the silver surface and increases its activity, particularly at higher coverage [40]. Additionally, XRD results from this study indicate that the Ag-Cs-Re/Al₂O₃ catalyst is mainly dominated by Ag (111) crystallites, leading to more carbonate species formation on the surface at ethylene-rich conditions (C₂H₄:O₂ = 4:1 in this experiment) [41,42]. Consequently, more subsurface oxygen can be stabilized in the Ag-Cs-Re/Al₂O₃ catalyst after the induction process. Considering that subsurface oxygen can stabilize the adsorption of C₂H₄ and O₂, and enhance the dissociation of O₂, it thereby promotes the epoxidation of ethylene [40,43]. The carbonates generated during the induction process can significantly enhance the reaction rate of ethylene epoxidation. It should be noted that subsurface oxygen can also increase the selectivity of ethylene. Recent literature reports the existence of subsurface oxygen species unique to EO production, which may be responsible for inducing elevated selectivity [25]. The Ag-Cs-Re/Al₂O₃ catalysts showed bond vibrational peaks at 842 cm⁻¹ in the infrared spectra of the catalysts, which is attributed to Al-O bonding on the surface, a similar peak has also been observed in the previous studies [44].

The DRIFTS results of Ag-Cs-Re/Al₂O₃ catalyst before and after induction with reacting gases under C₂H₄ atmosphere are shown in Fig. 7b. Stretching vibrational peaks of carbonates are also observed. Surface carbonates are also stable under ethylene atmosphere (after treatment). The adsorption peaks at 2100–1850 cm⁻¹, 1530–1360 cm⁻¹, and 1150–800 cm⁻¹ are both generated under C₂H₄ atmosphere, which are the vibrational absorption peaks of C—H and C=C bond in the ethylene.

3.3.4. Mechanism of induction

After systematical characterization of induced catalysts, it was found that catalysts prepared using the impregnation method with Ag (111) silver crystalline surfaces as the main catalysts could form carbonate species on the Ag surface induced by high temperature under reactive gas conditions (Fig. 8). The presence of carbonates could stabilize more sub-surface oxygen, promote the dissociative adsorption of C₂H₄ and O₂, benefit the process of ethylene epoxidation, and significantly increase the reaction rate with high selectivity.

3.4. Stability test for the silver catalyst after successful induction

With an increase in EO production rate with induction procedures for Ag/α-Al₂O₃, it is of great importance to examine whether the high EO activity could be stably maintained. The results are shown in Fig. 9. The EO production rate and selectivity were both stably maintained for 120 h after induction. The formation rate and selectivity of EO reached 1.65 × 10⁻² mol/h/g_{Ag} and 83 % at the 150th hour, respectively. No decrease in EO formation rate or selectivity was observed, suggesting that the successfully induced Ag/Al₂O₃ catalyst can maintain its EO activity over a long period of operation.

In general, increasing the temperature leads to an increase in the chemical reaction rate; however, it simultaneously decreases product selectivity, a phenomenon known as the seesaw effect. This occurs because, while the reaction rate increases with temperature, the reaction rate of its side reaction, deep oxidation, also increases, resulting in a decrease in selectivity for ethylene epoxidation [16,45–49]. Rojuechai, Chavadej, Schwank, Meeyoo [45] prepared an Ag/Au catalyst with a conversion of 1.8 % and a selectivity of 79.0 %, and Ren, Cheng, Li, Li, Dai, Sun, Cheng [19] prepared an Ag catalyst with a conversion of 11.5 % and a selectivity of 72.4 %. A comparison of different catalysts in the literature showed a significant negative correlation between conversion and selectivity. However, the simple induction process proposed in this study achieved dual success in conversion and selectivity, reaching 12.5 % and 84.4 %, respectively. As shown in the EO formation rate comparison in Fig. 10b, the EO formation rate after induction reached 2.17

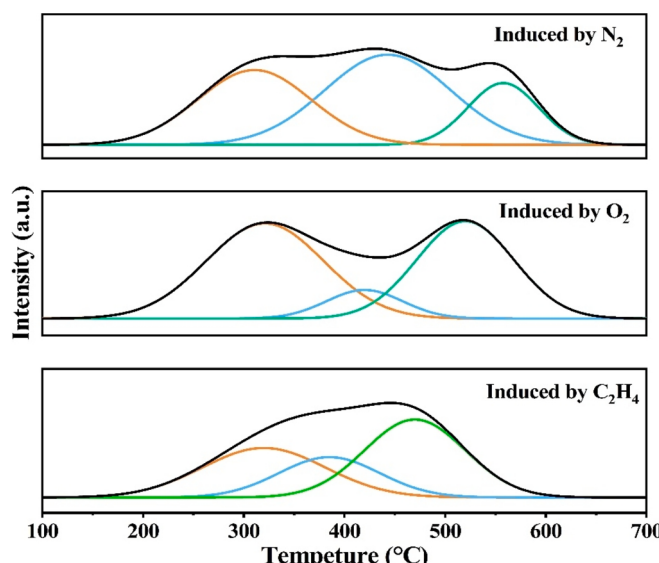


Fig. 6. O₂-TPD results for Ag-Cs-Re/Al₂O₃ catalyst induced with various gases at 260 °C.

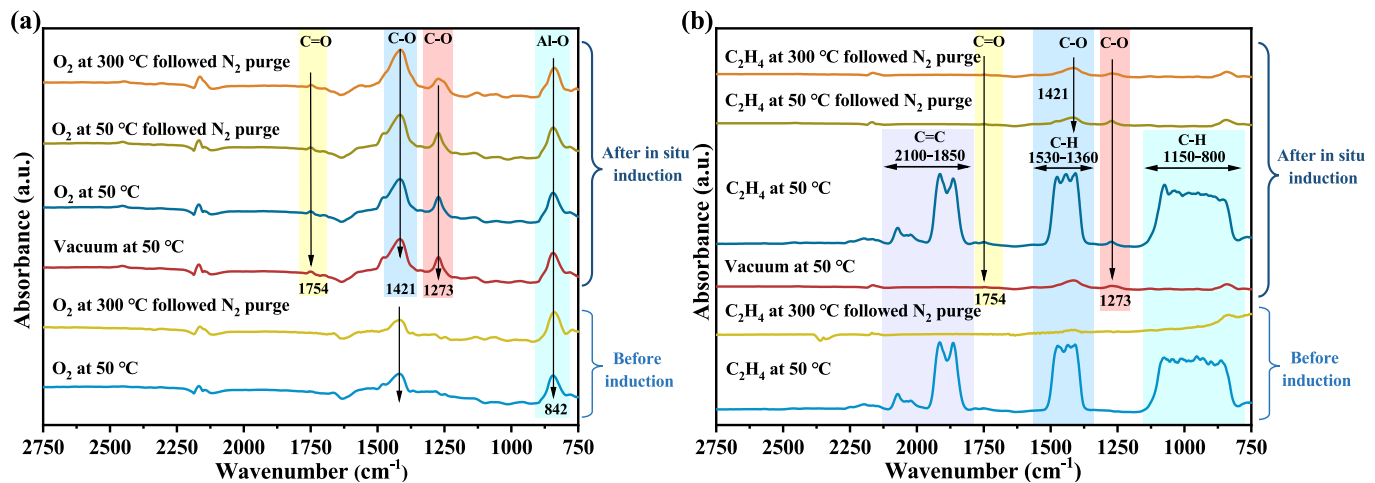


Fig. 7. DRIFTS result for O₂ and C₂H₄ adsorption for the Ag-Cs-Re/Al₂O₃ catalyst before and after *in-situ* induction with reacting gases.

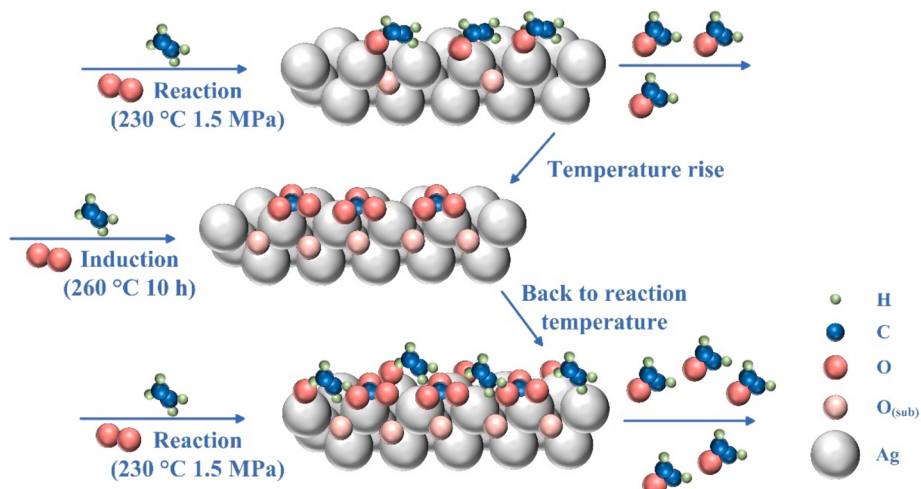


Fig. 8. Schematic illustration of silver catalyst gas-induced surface.

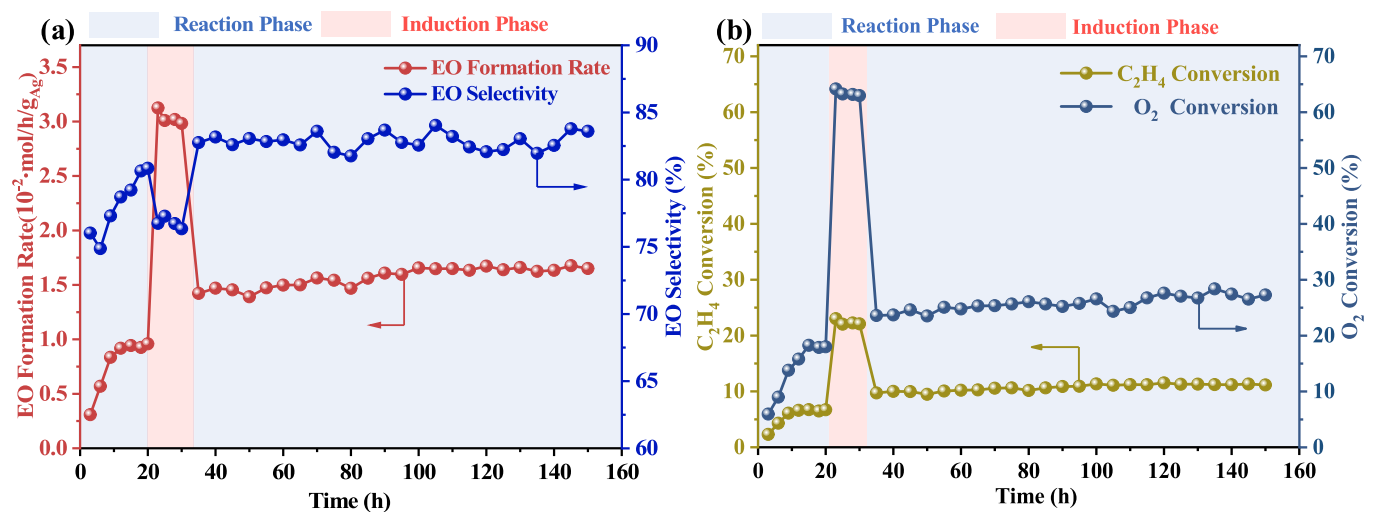


Fig. 9. Long period running performance of induced Ag/Al₂O₃ catalyst at reaction conditions of 230 °C, 1.5 MPa C₂H₄, 1.5 MPa O₂ and a gas hourly space velocity of 4200 mL·h⁻¹·g_{Ag}⁻¹.

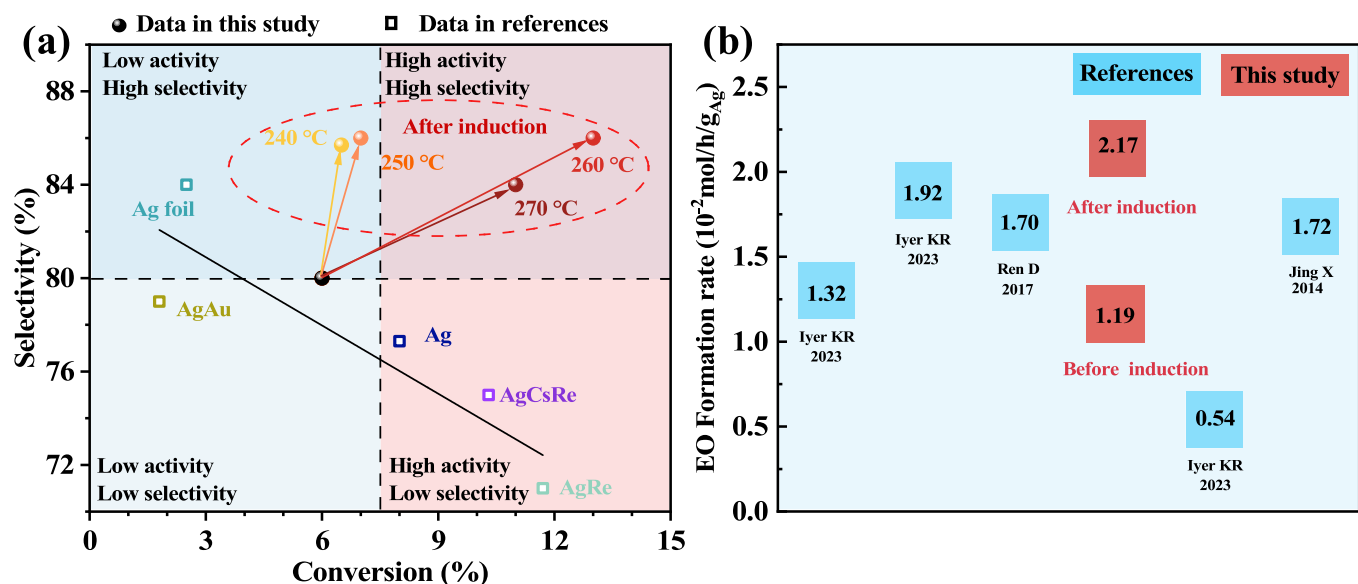


Fig. 10. The comparison of catalysis performance of induced Ag-Cs-Re/Al₂O₃ catalyst and Ag based catalysts in previous studies [19,27,45,46,48–50].

$\times 10^{-2}$ mol/h/g_{Ag}, which is 13 % higher than the highest reaction rate reported in some of the work in the literature [27,48–50]. In conclusion, this study presents a method to improve catalyst performance, enabling the efficient conversion of ethylene to EO through common catalyst preparation methods.

4. Conclusion

An induced behavior of 82 % higher activity for EO production over Ag-Cs-Re/Al₂O₃ catalysts was found at elevated temperatures in the presence of reaction gases. An induction temperature of 260 °C was identified as optimal for achieving a high EO production rate and selectivity simultaneously. Suitable atmospheres (e.g., O₂, C₂H₄, and fully reactive gases) are also necessary to conduct a successful induction. FESEM results indicated that the growth rate of silver particles in the reaction process may be attenuated when exposed to the reacting gases during induction. O₂-TPD analyses showed that more subsurface oxygen was generated using O₂ as the induction gas compared to N₂. In situ DRIFTS experiments demonstrated that the induction process produced C—O and C=O bond vibrations at 1273 cm⁻¹ and 1754 cm⁻¹, respectively, attributed to the vibrations of carbonates formed on the silver and carrier surfaces. The formation of carbonates under the reactive conditions facilitates the stabilization of more subsurface oxygen species. This stabilization promotes the adsorption and dissociation of O₂ and C₂H₄ on the reaction surface, greatly enhancing reaction activity. By utilizing the induced behavior of high ethylene oxide activity, the silver loading can be reduced. As the silver content decreases, the addition of precious metal promoters also decreases, significantly lowering the catalyst cost for producing ethylene oxide with silver catalysts and improving the economic efficiency of production.

CRedit authorship contribution statement

Xiaojun Lu: Writing – original draft. **Pei Zhang:** Methodology, Investigation. **Zhichao Deng:** Writing – review & editing, Data curation. **Chengyang He:** Visualization, Investigation. **Rui Zhang:** Writing – review & editing, Methodology, Formal analysis, Data curation.

Declaration of competing interest

The authors declare that they have no known competing financial interests or personal relationships that could have appeared to influence

the work reported in this paper.

Data availability

Data will be made available on request.

Acknowledgment

This work was supported by the National Science Foundation for Young Scientists of China (No. 22202165) and Wuhan Institute of Technology, China (20QD74 and CX2022057).

Appendix A. Supplementary material

Supplementary data to this article can be found online at <https://doi.org/10.1016/j.fuel.2024.133346>.

References

- Pinaeva L, Noskov AJPC. Prospects for the development of ethylene oxide production catalysts and processes. Pet Chem 2020;60:1191–206. <https://doi.org/10.1134/S096554412011016X>.
- Ren T, Patel M, Blok K. Olefins from conventional and heavy feedstocks: Energy use in steam cracking and alternative processes. Energy 2006;31(4):425–51. <https://doi.org/10.1016/j.energy.2005.04.001>.
- Chen Y, Wei J, Duyar MS, Ordovsky VV, Khodakov AY, Liu J. Carbon-based catalysts for Fischer-Tropsch synthesis. Chem Soc Rev 2021;50(4):2337–66. <https://doi.org/10.1039/DOSR00905A>.
- Zhang J, Dang L, Lai T, Yuan H, Zhang D, Gao G. Pathway modulation and substrate partitioning for CO₂-assisted hydration of ethylene oxide catalyzed by swellable poly(ionic liquids). Fuel 2024;355:129521. <https://doi.org/10.1016/j.fuel.2023.129521>.
- Yuan H, Dang L, Tang H, Wang B, Zhang J, Lai T, et al. Bi-functional phosphonium poly(ionic liquid)s catalyzed CO₂-promoted hydration of ethylene oxide. Fuel 2023;345:128210. <https://doi.org/10.1016/j.fuel.2023.128210>.
- Guo Y, Zhang J, Sun N, Ling L, Zhang R, Guo H, et al. Ethylene carbonate generated efficiently via ethylene oxide and CO₂ on the Li-MgO(100) surface based on the synergistic activation of bimetal without halogen. Fuel 2023;342:127823. <https://doi.org/10.1016/j.fuel.2023.127823>.
- Pu T, Tian H, Ford ME, Rangarajan S, Wachs IE. Overview of selective oxidation of ethylene to ethylene oxide by Ag catalysts. ACS Catal 2019;9(12):10727–50. <https://doi.org/10.1021/acscatal.9b03443>.
- Keijzer PH, Donoeva B, de Jong KP, de Jongh PE. Supported silver catalysts prepared via melt infiltration: synthesis, characterization and performance in selective hydrogenation. Catal Today 2021;375:393–400. <https://doi.org/10.1016/j.cattod.2020.03.017>.
- Montemore MM, van Spronsen MA, Madix RJ, Friend CM. O₂ activation by metal surfaces: implications for bonding and reactivity on heterogeneous catalysts. Chem Rev 2018;118(5):2816–62. <https://doi.org/10.1021/acs.chemrev.7b00217>.

- [10] Li H, Cao A, Nørskov JK. Understanding trends in ethylene epoxidation on group IB metals. *ACS Catal* 2021;11(19):12052–7. <https://doi.org/10.1021/acscatal.1c03094>.
- [11] Pu T, Setiawan A, Mosevitzky Lis B, Zhu M, Ford ME, Rangarajan S, et al. Nature and reactivity of oxygen species on/in silver catalysts during ethylene oxidation. *ACS Catal* 2022;12(8):4375–81. <https://doi.org/10.1021/acscatal.1c05939>.
- [12] Bukhtiyarov VI, Prosvirin IP, Kvon RI. Study of reactivity of oxygen states adsorbed at a silver surface towards C_2H_4 by XPS, TPD and TPR. *Surf Sci* 1994;320(1): L47–50. [https://doi.org/10.1016/0039-6028\(94\)00562-1](https://doi.org/10.1016/0039-6028(94)00562-1).
- [13] Bukhtiyarov VI, Nizovskii AI, Bluhm H, Hävecker M, Kleimenov E, Knop-Gericke A, et al. Combined in situ XPS and PTRMS study of ethylene epoxidation over silver. *J Catal* 2006;238(2):260–9. <https://doi.org/10.1016/j.jcat.2005.11.043>.
- [14] Rocha TCR, Oesterreich A, Demidov DV, Hävecker M, Zafeiratos S, Weinberg G, et al. The silver–oxygen system in catalysis: new insights by near ambient pressure X-ray photoelectron spectroscopy. *Phys Chem Chem Phys* 2012;14(13):4554–64. <https://doi.org/10.1039/C2CP22472K>.
- [15] Jones TE, Rocha TCR, Knop-Gericke A, Stampfli C, Schlögl R, Piccinin S. Thermodynamic and spectroscopic properties of oxygen on silver under an oxygen atmosphere. *Phys Chem Chem Phys* 2015;17(14):9288–312. <https://doi.org/10.1039/C5CP00342C>.
- [16] Jankowiak JT, Bartea MAJJC. Ethylene epoxidation over silver and copper–silver bimetallic catalysts: II. Cs and Cl promotion. *J Catal* 2005;236(2): 379–86. <https://doi.org/10.1016/j.jcat.2005.10.017>.
- [17] Serafin JG, Liu AC, Seyedmonir SRJC. ChemInform abstract: surface science and the silver-catalyzed epoxidation of ethylene: an industrial perspective. *ChemInform* 1998. <https://doi.org/10.1002/chin.199840309>.
- [18] R.P. Nielsen, Rochelle JHL. Catalyst for production of ethylene oxide. US; 1976.
- [19] Ren D, Cheng G, Li J, Li J, Dai W, Sun XX, et al. Effect of rhenium loading sequence on selectivity of Ag–Cs catalyst for Ethylene Epoxidation. *Catal Lett* 2017. <https://doi.org/10.1007/s10562-017-2211-5>.
- [20] Xu H, Zhu L, Nan Y, Xie Y, Cheng D. Revisit the role of metal dopants in enhancing the selectivity of Ag-catalyzed ethylene epoxidation: optimizing oxophilicity of reaction site via cocatalytic mechanism. *ACS Catal* 2021;11(6):3371–83. <https://doi.org/10.1021/acscatal.0c04951>.
- [21] Jingfa D, Jun Y, Shi Z, Xiaohong Y. Promoting effects of Re and Cs on silver catalyst in ethylene epoxidation. *J Catal* 1992;138(1):395–9. [https://doi.org/10.1016/0021-9517\(92\)90033-E](https://doi.org/10.1016/0021-9517(92)90033-E).
- [22] He C, Lu X, Liu Y, Yan Z, Zhang R, Liu X. Stability enhancement for silver catalyst in ethylene epoxidation by support treatment. *Catal Commun* 2023;178:106669. <https://doi.org/10.1016/j.catcom.2023.106669>.
- [23] Sun L, Huang H, Che P, Lin Q, Lian K, Li J, et al. In situ discovery on the formation of supported silver catalysts for ethylene epoxidation. *Adv Powder Technol* 2022; 33(9):103732. <https://doi.org/10.1016/j.japt.2022.103732>.
- [24] A. J. F. van Hoof EARH, A. P. van Bavel, H. Friedrich, and E. J. M. Hensen. Structure Sensitivity of Silver-Catalyzed Ethylene Epoxidation. *ACS Catal*. 2019;9 (11). Doi: 10.1021/acscatal.9b02720.
- [25] Chen D, Chen L, Zhao Q-C, Yang Z-X, Shang C, Liu Z-P. Square-pyramidal subsurface oxygen [Ag₆OAg] drives selective ethene epoxidation on silver. *Nat Catal* 2024;7(5):536–45. <https://doi.org/10.1038/s41929-024-01135-2>.
- [26] van Hoof AJF, Filot IAW, Friedrich H, Hensen EJM. Reversible restructuring of silver particles during ethylene epoxidation. *ACS Catal* 2018;8(12):11794–800. <https://doi.org/10.1021/acscatal.8b03331>.
- [27] Iyer KR, Bhan AJJC. Particle size dependence of ethylene epoxidation rates on Ag/a-Al₂O₃ catalysts: Why particle size distributions matter. *J. Catal.* 2023. Doi: 10.1016/j.jcat.2023.02.008.
- [28] Van dR, J. E., Kanungo S, Welling TAJ, Versluijs-Helder M, Nijhuis TA, De Jong KP, et al. Preparation and particle size effects of Ag/ α -Al₂O₃ catalysts for ethylene epoxidation. *J Catal* 2017;356:65–74. Doi: 10.1016/j.jcat.2017.10.001.
- [29] And SL, Bartea MA. Formation of a Stable Surface Oxametallacycle that Produces Ethylene Oxide. *ACS Catal* 2001. <https://doi.org/10.1021/ja0118136>.
- [30] Kim Y-C, Park N-C, Shin J-S, Lee SR, Lee YJ, Moon DJ. Partial oxidation of ethylene to ethylene oxide over nanosized Ag/ α -Al₂O₃ catalysts. *Catal Today* 2003;87(1): 153–62. <https://doi.org/10.1016/j.cattod.2003.09.012>.
- [31] Serafin JG, Liu AC, Seyedmonir SR. Surface science and the silver-catalyzed epoxidation of ethylene: an industrial perspective. *J Mol Catal A: Chem* 1998;131 (1):157–68. [https://doi.org/10.1016/S1381-1169\(97\)00263-X](https://doi.org/10.1016/S1381-1169(97)00263-X).
- [32] Atkins M, Couves J, Hague M, Sakakini BH, Waugh KC. On the role of Cs, Cl and subsurface O in promoting selectivity in Ag/ α -Al₂O₃ catalysed oxidation of ethene to ethene epoxide. *J Catal* 2005;235(1):103–13. <https://doi.org/10.1016/j.jcat.2005.07.019>.
- [33] Dellamorte JC, Lauterbach J, Bartheau MA. Effect of preparation conditions on Ag catalysts for ethylene epoxidation. *Top Catal* 2010;53(1):13–8. <https://doi.org/10.1007/s11244-009-9440-9>.
- [34] Bukhtiyarov VI, Knop-Gericke A. Chapter 9:Ethylene Epoxidation over Silver Catalysts. 2011.
- [35] Force EL, Bell ATJJOC. Infrared spectra of adsorbed species present during the oxidation of ethylene over silver. *J. Catal.* 1975;38(1-3):440-60. Doi: 10.1016/0021-9517(75)90107-4.
- [36] Kirschbaum C, Said EM, Greis K, Mucha E, Gewinner S, Schöllkopf W, et al. Resolving Sphingolipid Isomers Using Cryogenic Infrared Spectroscopy. *Angew Chem Int Ed* 2020;59(32):13638–42. <https://doi.org/10.1002/anie.202002459>.
- [37] Mu J, Perlmutter DD. Thermal decomposition of carbonates, carboxylates, oxalates, acetates, formates, and hydroxides. *Thermochim Acta* 1981;49(2): 207–18. [https://doi.org/10.1016/0040-6031\(81\)80175-X](https://doi.org/10.1016/0040-6031(81)80175-X).
- [38] Bulushev DA, Paukshtis EA, Nogin YN, Bal'zhinimaev BS. Transient response and infrared studies of ethylene oxide reactions on silver catalysts and supports. *Appl Catal*, A 1995;123(2):301–22. [https://doi.org/10.1016/0926-860X\(94\)00221-5](https://doi.org/10.1016/0926-860X(94)00221-5).
- [39] Podobiński J, Datka J. Basic sites on alumina with preadsorbed ethanol and ammonia—an IR study. *Molecules* 2024;29(8):1726. <https://doi.org/10.3390/molecules29081726>.
- [40] Xu Y, Greeley J, Mavrikakis MJJC. Effect of Subsurface Oxygen on the Reactivity of the Ag(111) Surface. *J. Am. Chem. Soc.* 2005;127(37):12823. Doi: 10.1021/ja043727m.
- [41] Isegawa K, Ueda K, Amemiya K, Mase K, Kondoh H. Formation and behavior of carbonates on Ag(110) in the presence of ethylene and oxygen. *J Phys Chem C* 2021;17:125. <https://doi.org/10.1021/acs.jpcc.0c11597>.
- [42] Kazuhisa Isegawa KU, Satoru Hiwasa, Kenta Amemiya, Kazuhiko Mase, Hiroshi Kondoh. Formation of Carbonate on Ag(111) under Exposure to Ethylene and Oxygen Gases Evidenced by Near Ambient Pressure XPS and NEXAFS. *Chem. Lett.* 2019;48(2). Doi: 10.1246/cl.180891.
- [43] Linic S, Bartheau MA. Construction of a reaction coordinate and a microkinetic model for ethylene epoxidation on silver from DFT calculations and surface science experiments. *J Catal* 2003;214(2):200–12. [https://doi.org/10.1016/S0021-9517\(02\)00156-2](https://doi.org/10.1016/S0021-9517(02)00156-2).
- [44] Debnath S, Jorewitz M, Asmis KR, Müller F, Stückrath JB, Bischoff FA, et al. Infrared photodissociation spectroscopy of (Al₂O₃)²5FeO⁺: influence of Fe-substitution on small alumina clusters. *Phys Chem Chem Phys* 2022;24(35): 20913–20. <https://doi.org/10.1039/D2CP02938C>.
- [45] Rojuechai S, Chavadej S, Schwank JW, Meeeyo VJCC. Catalytic activity of ethylene oxidation over Au, Ag and Au–Ag catalysts: Support effect. *Catal Commun* 2007;8(1):57–64. <https://doi.org/10.1016/j.catcom.2006.05.029>.
- [46] Chen BWJ, Wang B, Sullivan MB, Borgna A, Zhang JJAC. Unraveling the Synergistic Effect of Re and Cs Promoters on Ethylene Epoxidation over Silver Catalysts with Machine Learning-Accelerated First-Principles Simulations. *ACS Catal.* 2022(4):12. Doi: 10.1021/acscatal.1c05419.
- [47] Diao W, DiGiulio CD, Schaaf MT, Ma S, Monnier JR. An investigation on the role of Re as a promoter in Ag_xRe/ α -Al₂O₃ high-selectivity, ethylene epoxidation catalysts. *J Catal* 2015;322:14–23. <https://doi.org/10.1016/j.jcat.2014.11.007>.
- [48] Deng J, Yang J, et al. Promoting effects of Re and Cs on silver catalyst in ethylene epoxidation. *J Catal* 1992. [https://doi.org/10.1016/0021-9517\(92\)90033-E](https://doi.org/10.1016/0021-9517(92)90033-E).
- [49] Ren D, Cheng G, Li J, Li J, Dai W, Sun X, et al. Effect of rhenium loading sequence on selectivity of Ag–Cs catalyst for ethylene epoxidation. *Catal Lett* 2017;147(12): 2920–8. <https://doi.org/10.1007/s10562-017-2211-5>.
- [50] Jing X, Wang H, Chen H, Huang J, Li Q, Sun D. Biosynthesized Ag/ α -Al₂O₃ catalyst for ethylene epoxidation: the influence of silver precursors. *RSC Adv* 2014;4(52): 27597–603. <https://doi.org/10.1039/C4RA03312D>.